ISBN: 978-3-95450-231-8 ISSN: 2673-5490 doi: 10.18429/JACoW-IPAC2023-MOPL172

PROTOTYPING OF A DISK-LOADED STRUCTURE FOR MUON ACCELERATION

K. Sumi*, Y. Ibaraki, T. Iijima, K. Inami, Y. Sue, M. Yotsuzuka
Nagoya University, Nagoya, Aichi, Japan
H. Ego, T. Mibe, M. Otani, N. Saito, M. Yoshida
High Energy Accelerator Research Organization (KEK), Tsukuba, Ibaraki, Japan
Y. Kondo, Japan Atomic Energy Agency (JAEA), Tokai, Naka, Ibaraki, Japan
Y. Nakazawa, Ibaraki University, Mito, Ibaraki, Japan
Y. Takeuchi, Kyushu University, Fukuoka, Japan
H. Yasuda, University of Tokyo, Tokyo, Japan

Abstract

The muon linear accelerator is under development at J-PARC for precise measurement of muon anomalous magnetic moment and electric dipole moment. Four 2592 MHz disk-loaded structures (DLSs) operating in the TM01-2π/3 mode take charge of the acceleration of high-velocity muon from 70% to 94% of the speed of light. They have disk-iris apertures tapered to generate a quasi-constant gradient of 20 MV/m. Gradual variation in disk space at each cell is one of the structural features of the DLS for muon to synchronize the accelerating phase with the changing speed of muon. Therefore, the dimensions of both end cells are significantly different. Two prototypes of RF couplers and two 9-cell reference cavities with shapes of the end cells of the DLS at the first stage have been fabricated and tested. We validate our design RF parameters and establish a method for tuning the DLS in this paper.

INTRODUCTION

At J-PARC, an experiment is planned to investigate the puzzle of the muon anomalous magnetic moment [1] and to search for the muon electric dipole moment, using novel techniques, especially a low-emittance muon beam [2]. The required beam quality includes a low transverse normalized emittance of approximately 1.5π mm mrad and a small momentum spread of less than 0.1% in root-mean-square at 300 MeV/c. To achieve the desired beam quality, an unprecedented muon linear accelerator is under development [3, 4]. Four muon-dedicated disk-loaded structures (DLSs) are responsible for accelerating the muons from 70% to 94% of the speed of light and have a gradual variation in the disk spacing to synchronize the phase velocity of the electromagnetic field in the DLS with the varying muon velocity. In this paper, we report on the fabrication and RF measurement results for the DLS prototypes.

MUON-DEDICATED STRUCTURE

Table 1 summarizes the main properties of the DLSs, and more details about the design can be found in [5, 6]. The disk spacing is proportional to the muon velocity for synchronization conditions, as described in the introduction. The diameter of the iris apertures is also different and tapered to obtain a quasi-constant accelerating gradient. Therefore, the dimensions of the cells differ significantly at the upstream and downstream ends. Especially in the DLS at the first stage, where the muon velocity is lowest, the disk spacing is narrow and the variation is large. To verify the feasibility of this design, prototypes for the upstream and downstream ends of the first DLS were fabricated using oxygen-free copper.

Table 1: Main Parameters of the DLS Section

Stage	1st	2nd	3rd	4th
Structure type	Disk-loaded traveling-wave quasi-Constant Gradient type			
Operating frequency	2592 MHz			
Accelerating mode	TM01-2π/3			
Muon velocity [%c]	70-82	82-89	89-92	92-94
# of regular cells	63	63	60	60
Length [m]	1.97	2.21	2.23	2.30
Input RF power [MW]	~40			
Gradient [MV/m]	19.6	20.8	21.3	21.4

PROTOTYPING

Figure 1(a) shows the cross-sectional view of the fabricated prototypes of the first DLS, which include RF couplers and 9-cell reference cavities for both upstream and downstream. Each coupler is composed of one coupler cell that couples with a single rectangular waveguide and two regular cells. Meanwhile, each reference cavity is a constant-impedance structure consisting of eight brazed regular cells part and two non-brazed half cells. All regular cells have identical dimensions to the second cell from upstream or downstream as shown in Table 2. This modification was made to validate the RF properties of the regular cells by measuring them using the reference cavities and to perform Nodal shift measurements using precisely tuned brazed cells. The regular cells in the reference cavities are cup-shaped structures integrating a disk and cylinder to simplify the construction process and reduce costs as shown in Fig. 1(b). RF measurement setups are shown in Fig. 1(c), (d), and (e), all conducted under a nitrogen atmosphere, with the results converted to the values under a vacuum.

* ksumi@hepl.phys.nagoya-u.ac.jp

ISBN: 978-3-95450-231-8 ISSN: 2673-5490 doi: 10.18429/JACoW-IPAC2023-MOPL172

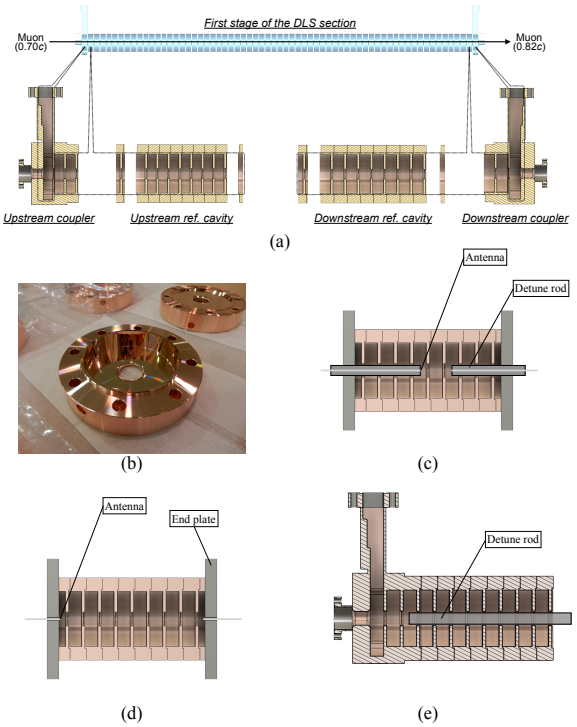

Figure 1: Schematic diagrams and photographs of prototypes and measurement setups: (a) Cross-sectional view of the fabricated cavities, (b) Fabricated regular cell, (c) $\pi/2$ mode measurement setup, (d) Dispersion curve measurement setup, and (e) Nodal shift measurement setup.

Table 2: Parameters of the Regular Cells

Parameters	Upstream	Downstream
Muon velocity [%c]	69.5	81.7
Cell length [mm]	26.935	31.436
Iris aperture [mm]	25.875	22.620
Cylinder diameter [mm]	92.332	90.874
Disk thickness [mm]	5	
$\pi/2$ mode frequency [MHz]	2574.8	2582.5
Coupling coefficient	0.0263	0.0147

Reference Cavities

The cavities were brazed after precision machining, $2\pi/3$ mode frequency measurement, and frequency tuning. The brazing process was successful with little change in $2\pi/3$ mode frequency before and after brazing, and the brazed cavities passed vacuum and cooling water pressure tests. The $\pi/2$ mode frequencies of each cell were measured in the setup shown in Fig. 1(c). Although the dimensions of each cell were designed to be identical, manufacturing errors caused frequency variation. To suppress the variation, dimpling, a technique to reduce the inner diameter of the cavity by pushing it from the outside, was conducted as the first step of the tuning process. As a result, the variation was sufficiently suppressed to less than 0.05 MHz at the peak-to-peak value, as shown in Fig. 2. After that, the $2\pi/3$ mode frequency was measured in the setup shown in Fig. 1(d), and final tuning was performed to reach 2592.00(5) MHz. The measured frequencies in the dispersion curve are presented in Fig. 3, and the coupling coefficients were as expected [6].

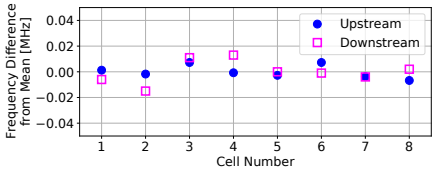

Figure 2: $\pi/2$ mode frequency as the difference from the average of 8 cells in each reference cavity.

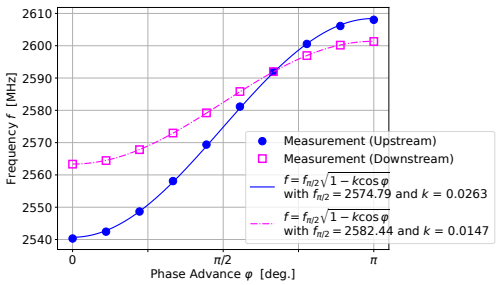

Figure 3: Dispersion curve of the reference cavities.

Table 3 presents a comparison of the quality factor Q for the $2\pi/3$ mode in the reference cavities obtained from simulations conducted by SUPERFISH [7] and measurements. The reduction due to the end plates was estimated by the simulation to be 13.0% for upstream and 12.3% for downstream. The measured Q for the upstream and downstream were 96.4% and 91.6% of their respective simulated values. It is unclear why the drop is larger for the downstream. One possibility is that the end plates or half-cell contacts are insufficient.

Table 3: Comparison of the Simulated and Measured Quality Factor

Parameters	Upstream	Downstream
Simulation w/o end plate	11314	12785
Simulation w/ end plate	9840.2	11210
Measurement w/ end plate	9490.2	10263

The shunt impedance was also evaluated using bead pull measurements. Figure 4 shows the measured frequency shifts of the reference cavities while a spherical copper bead with a diameter of 3.2 mm moved along the axis. The data from the central three cells were extracted to reduce the effect of the end plates and the Fourier series coefficient for the $2\pi/3$ mode $A_{2\pi/3}$ calculated as shown in Fig. 5. The shunt impedance per unit length is obtained using $A_{2\pi/3}$ as the following equation,

$$Z = \frac{{A_{2\pi/3}}^2 QL}{4\pi^2 \varepsilon a^3 f_0^2}, \quad (1)$$

ISBN: 978-3-95450-231-8 ISSN: 2673-5490 doi: 10.18429/JACoW-IPAC2023-MOPL172

where L is the length of a reference cavity, ε is the permittivity of nitrogen gas, and f_0 is the resonant frequency of the reference cavity. The results of the shunt impedance evaluation are summarized in Table 4. The measured Z tended to be slightly larger than expected for both cavities, but it also appears that the measurement uncertainty was large.

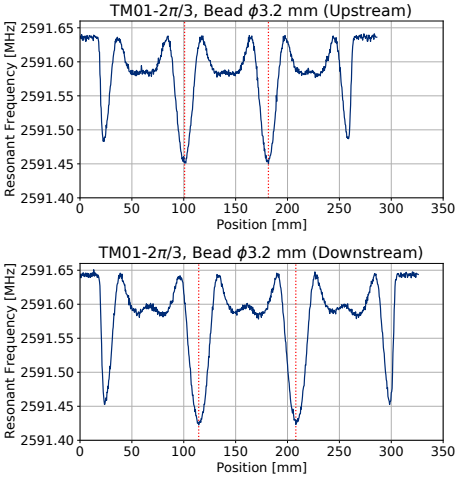

Figure 4: Frequency shift of the reference cavities by the bead pull measurement.

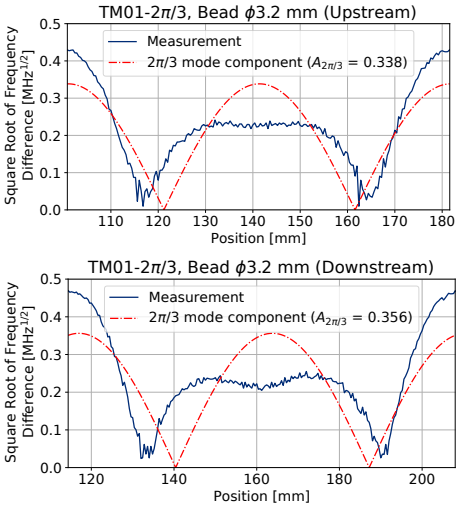

Figure 5: Axial field distributions and Fourier analysis results for the central three cells of the reference cavities.

Table 4: Comparison of the Simulated and Measured Shunt Impedance

Parameters	Upstream	Downstream
$A_{2\pi/3}$	0.338	0.356
Measured Q in this setup	9136.3/.870	10362/.877
Measured shunt impedance Z [MΩ/m]	30.3	44.1
Simulated shunt impedance [MΩ/m]	27.56	43.14

Couplers

The coupler was tuned using the Kyhl method [8]. Reflection measurements determined the iris width and cylinder diameter, which relates the coupling with the rectangular waveguide and resonant frequency, respectively. The frequency was further tuned by dimpling after brazing, and the accuracy of the phase difference between when the coupler cell is detuned and when the second cell is detuned was achieved at approximately 0.5°. Following coupler tuning, phase advance measurements were also conducted using the Nodal shift method with the tuned reference cavity as shown in Fig. 1(e). However, the results in Fig. 6 show that the phase advance at some cells differed significantly from 120°. It is believed that this discrepancy was due to imperfect detuning by the rod, which resulted in non-optimal tuning.

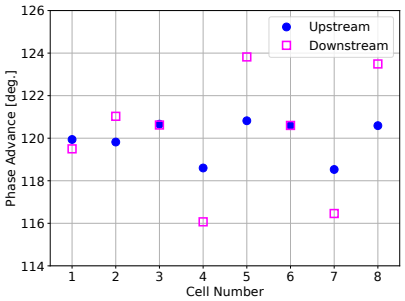

Figure 6: Phase advance measured by Nodal shift method.

SUMMARY AND PROSPECTS

In order to realize muon acceleration using the unprecedented muon-dedicated DLS, we fabricated couplers and reference cavities and evaluated their RF characteristics. Frequency and coupling coefficient agreed well, but Q and Z showed deviation. Despite using the Kyhl method for coupler tuning, Nodal shift measurements revealed phase shifts. To further understand the magnitude and source of the error for Z, additional measurements are considered using an alternative bead or a plunger. To understand this situation we will first calculate an equivalent circuit model. Based on these results, we will further investigate beam dynamics that are closer to the actual situation.

ACKNOWLEDGEMENTS

This work is supported by JSPS KAKENHI Grant Numbers JP18H03707, JP18H05226, JP20H05625, 21K18630, 21H05088, 22H00141, 22J20870, 22KJ1594, JST FOREST Program (Grant Number JPMJFR212O), and the natural science grant of the Mitsubishi Foundation. This paper is based on results obtained from a project commissioned by the New Energy and Industrial Technology Development Organization (NEDO). The authors would like to thank MITSUBISHI HEAVY INDUSTRIES MACHINERY SYSTEMS, LTD. for providing the fabrication and RF measurements.

ISBN: 978-3-95450-231-8 ISSN: 2673-5490 doi: 10.18429/JACoW-IPAC2023-MOPL172

REFERENCES

[1] A. Keshavarzi, K. S. Khaw, and T. Yoshioka, "Muon $g-2$: A review", *Nucl. Phys. B*, vol. 975, p. 115675, 2022. doi:10.1016/j.nuclphysb.2022.115675

[2] M. Abe *et al.*, "A new approach for measuring the muon anomalous magnetic moment and electric dipole moment", *Prog. Theor. Exp. Phys.*, vol. 2019, p. 053c02, 2019. doi:10.1093/ptep/ptz030

[3] M. Otani, "First muon acceleration and muon linear accelerator for measuring the muon anomalous magnetic moment and electric dipole moment", *Prog. Theor. Exp. Phys.*, vol. 2022, p. 052C01, 2022. doi:10.1093/ptep/ptac067

[4] Y. Kondo *et al.*, "The Muon Linac Project at J-PARC", in *Proc. 31st Linear Accel. Conf.*, Aug.-Sep. 2022, pp. 636-641. doi:10.18429/JACoW-LINAC2022-WE1AA05

[5] K. Sumi *et al.*, "Design and beam dynamics study of disk-loaded structure for muon LINAC", *J. Phys. Conf. Ser.*, vol. 2040, p. 012038, 2023. doi:10.1088/1742-6596/2420/1/012038

[6] K. Sumi *et al.*, "Design of coupler cells in the disk-loaded structure for the muon LINAC", in *Proc. 19th Annu. Meet. of Particle Accelerator Society of Japan*, Oct. 2022, pp. 202-206.

[7] J. H. Billen and L. M. Young, "Poisson Superfish", LA-UR-96-1834, 1996.

[8] E. P. Westbrook, "Microwave impedance matching of feed waveguides to the disk-loaded accelerator structure operating in the $2\pi/3$ mode", SLAC-TN-63-103, 1963.